Numerical simulation of a laboratory reception plate using finite elements

Steffi Reinhold[1,2], Carl Hopkins[1], Berndt Zeitler[2]

[1] *Acoustics Research Unit, School of Architecture, University of Liverpool, Liverpool L69 7ZN, E-Mail:steffi.reinhold@liverpool.ac.uk and carl.hopkins@liverpool.ac.uk*

[2] *University of Applied Sciences Stuttgart, 70174 Stuttgart, E-Mail: berndt.zeitler@hft-stuttgart.de*

Introduction

Sound transmission from building machinery is a potential cause of annoyance in residential buildings. Many types of machinery inject significant structure-borne sound power in the low frequency range. This research concerns the characterisation of structure-borne sound sources that are fixed to a heavyweight wall or floor. When the structure-borne sound source is installed in a heavyweight building there are errors in quantifying the structure-borne sound power due to the fact that the individual building components are rigidly connected to other building components [1,2]. However, structure-borne sound power input from machinery into heavyweight walls or floors can be quantified in the laboratory using the isolated reception plate [3] as described in EN 15657-1 [4]. Data obtained from this method can be used for the prediction of sound transmission (EN 12354-5 [5]) to nearby rooms.

This paper focuses on the development of two deterministic models of a heavyweight reception plate using Finite Element Methods (FEM) with ABAQUS software: (1) an idealised model of an isolated plate with free boundary conditions and (2) a detailed model of the reception plate in the laboratory at Stuttgart which incorporates a viscoelastic material around the boundaries to increase the damping. These FEM models are compared and validated against experimental results. A comparison of the direct injected power and reception plate power is made for harmonic point force excitation at different positions on the plate surface. The validated detailed model is used to assess different sampling strategies for vibration measurements needed to calculate the structure-borne sound power. This leads to a proposal for a weighting factor that minimises the errors and the number of measurement positions.

Measurements and simulation

Reception plate test rig

Figure 1 shows the heavyweight reception plate test rig in the laboratory at Stuttgart. The main components are the three, decoupled, perpendicular concrete plates which are supported around the edges by viscoelastic material with a high internal loss factor. Each plate is 100 mm thick and their area is in a range from 5.34 to 6.85 m². The vertical plates are held in place with six anchoring supports on each plate. Measurements of the structural reverberation time indicate that the total loss factor of all three plates is similar.

To create the most accurate FEM model, material properties are required. For the concrete plate the Young's modulus was calculated to be 25.9E9 N/m² from the measured quasi-longitudinal wave velocity on the reception plate [6,7]. The dynamic stiffness of the viscoelastic material (Sylomer) was obtained by measuring the mass-spring resonance frequency according to EN 29052-1 [8] giving a spring stiffness of 271004 N/m on a 0.1 x 0.1 m FEM element size with a loss factor of 0.61 determined at the resonance frequency from the half-power bandwidth. A previous conference contribution [9] describes the investigations of the material properties in more detail. In this paper, the FEM models and experimental validation are restricted to the horizontal plate.

Figure 1: Reception plate test rig at Stuttgart.

Experimental Modal Analysis

The first step was to identify the modal characteristics of the horizontal reception plate using Experimental Modal Analysis (EMA). To ensure that closely coupled modes or repeated roots are also resolved, a roving hammer excitation and multiple reference responses was conducted to obtain the frequency response functions. A 21 by 29 point measurement grid was used over the surface of the reception plate (size: 2.0 m by 2.8 m) with a total of 609 grid points.

The post processing of the vibration data was carried out by multiple reference curve fitting for all measured sets of frequency response functions (MDOF polynomial fit method). The lowest 13 mode shapes and eigenfrequencies of the horizontal reception plate obtained from the post processing are shown in Figure 2.

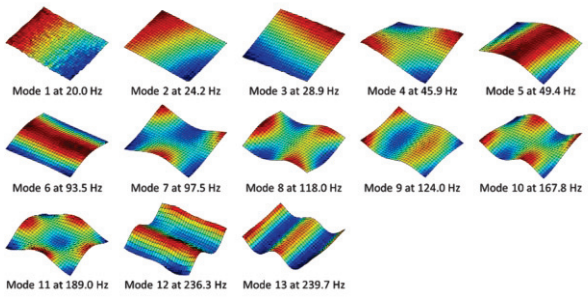

Figure 2: Experimental mode shapes: lowest 13 mode shapes and eigenfrequencies from EMA on the horizontal reception plate.

Reception plate method with FEM

The reception plate method described in EN 15657-1 [4] is used to quantify the structure-borne sound power input in the FEM model. This uses a power balance approach for a steady-state source. The source power equals the plate power of bending waves. The single-frequency velocity data from FEM is averaged to give one-third octave bands and the plate power is determined using

$$W_{\mathrm{rec}} = \omega m \eta \overline{\overline{v}}^2 \tag{1}$$

where ω is the angular frequency, m is the mass of the reception plate, η, is the total loss factor of the reception plate and $\overline{\overline{v}}^2$ is the spatial-average mean-square velocity.

The real part of the complex injected power which is delivered to the receiver can be calculated from the complex force, $\underline{F}$, and velocity, $\underline{v}$, at the driving-point.

$$W_{\mathrm{inj}} = \frac{1}{2}\mathrm{Re}\left[\underline{F}^* \underline{v}\right] \tag{2}$$

where * indicates the complex conjugate. In this paper, the reception plate power (1) is compared with the injected power (2).

Simulation with finite elements

To see the effect of the viscoelastic material around the edges two FEM models were created of the horizontal reception plate (see Figure 3): (1) an idealized representation using an isolated plate with free boundary conditions (referred to as FEM FFFF) and (2) a realistic representation of the plate which is supported around its boundaries by viscoelastic material (referred to as FEM Sylomer). For the FEM models thin triangular shell elements with three nodes (STRI3) are used with element dimensions $< \lambda_B / 8$ over the frequency range of interest. The concrete material properties in both FEM models use the measured Young's modulus (25.9E9 N/m²), the estimated Poisson's ratio (0.3), density (2300 kg/m³) and internal loss factor (0.005) [4,7].

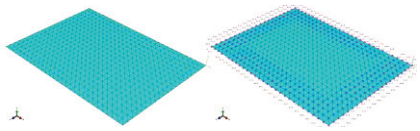

Figure 3: FEM models: FEM FFFF (left) and FEM Sylomer (right).

The viscoelastic material around the boundaries of the FEM model is considered as spring-dashpot elements with grounded connections to the reception plate. The measured spring stiffness and damping coefficient values are divided by four because two connected STRI3 elements can be considered as a square-shaped mass with four spring supports. The stiffness for these springs in parallel adds in series so the spring is applied to each of the four nodes. This gives spring-dashpot values of 67751 N/m for the spring stiffness and 124.35 for the dashpot coefficient. These are applied at each node in an area of 2.41 m² around the boundaries of the plate giving a total of 360 spring-dashpot elements.

The internal losses of materials relate to the structural damping, γ, in ABAQUS FEM models. The relationship with the internal loss factor, η_{int}, and the critical damping, ζ, ratio is given by

$$\gamma = \eta_{\mathrm{int}} = 2\zeta \tag{3}$$

To solve steady-state dynamic vibration response in the frequency domain a direct steady-state dynamic analysis (exact and most accurate solution) is carried out for free and forced vibrations with damping and performed with an applied harmonic force load. Both models consider the *in vacuo* situation (i.e. no radiation coupling). FEM analysis is carried out with a frequency resolution of 0.001 Hz.

Results

Measured and simulated loss factor

For the loss factor the simulated results are compared against the measured results in Figure 4. The loss factor obtained from measured structural reverberation times (black solid line with 95 % confidence interval) and measured driving-point mobilities using half-power bandwidth from five randomly distributed positions (blue asterisks) show close agreement. The loss factor of the reception plate determined using the driving-point mobility in FEM (red diamonds) shows good agreement with the experimental loss factor. This indicates that the damping from the viscoelastic material has been correctly incorporated in the FEM model.

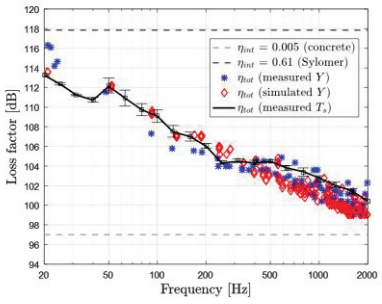

Figure 4: FEM Sylomer model: numerical and experimental loss factor.

Validation of FEM models against EMA

The two FEM models are validated against EMA measurements by considering the percentage error between two sets of natural frequencies, known as Natural Frequency Deviation (NFD) and the statistical indicator of the degree of correlation between two sets of mode shapes, known as the Modal Assurance Criterion (MAC).

Figure 5 shows the NFD results of the FEM models. For the FEM FFFF model, the first three FEM eigenfrequencies are whole body modes with nearly zero frequency and a zero stiffness matrix and these modes are not in agreement with EMA. However, the FEM Sylomer model has three whole body modes with non-zero frequency and a stiffness matrix

which is non-zero due to the fact that the plate is restrained at the boundaries by the viscoelastic material. There is close agreement with EMA for the natural frequencies of the six presented mode pairs above 100 Hz for the FEM FFFF model and for all 13 corresponding natural frequencies in a frequency range from 20 to 250 Hz for the FEM Sylomer model.

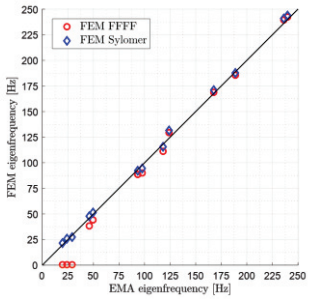

Figure 5: NFD values for corresponding mode pairs below 250 Hz.

The MAC results for both FEM models are shown in Figures 6 and 7. The FEM FFFF and Sylomer models show high correlation with EMA at and above the fourth mode up to the 13th mode. It is only for the FEM Sylomer model that strong correlation is achieved with the first three rigid body modes. This demonstrates that the viscoelastic material has been successfully incorporated into the FEM model and that the simplified model of a reception plate with free boundary conditions is unsuitable at low frequencies.

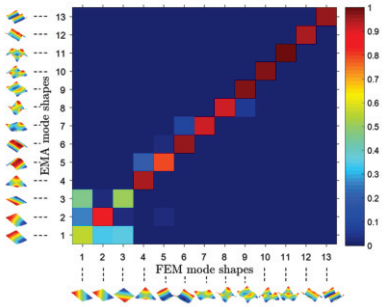

Figure 6: MAC values (mode shapes from FEM FFFF model and EMA).

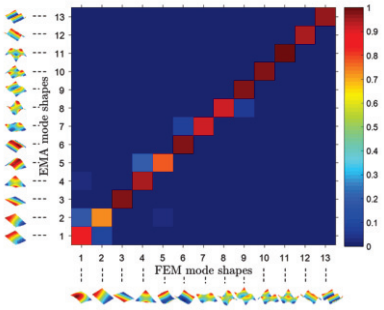

Figure 7: MAC values (mode shapes from FEM Sylomer model and EMA).

Numerical experiments with FEM

The comparison between direct injected power and reception plate power of both FEM models is shown in Figures 8 and 9 where both powers are obtained from five randomly distributed point force excitations. In these FEM calculations the reception plate power is determined using the velocity of all 2337 elements.

The FEM FFFF model shows close agreement (± 1 dB) between the direct injected power and the reception plate power when there is predicted at least one mode in each one-third octave band. Below 31.5 Hz there are differences of > 3 dB which are due to the simplistic assumptions of an isolated plate with free boundaries which leads to low damping and low mode counts in each band. In contrast, for the FEM Sylomer model there is close agreement (± 1 dB) between 20 Hz and 2000 Hz where modes occur. Although there were only whole body modes in the 20 and 25 Hz bands, the reception plate method still shows close agreement. The damping from the viscoelastic material is beneficial in the low-frequency bands below 100 Hz where the modes are sparse as it increases the modal overlap.

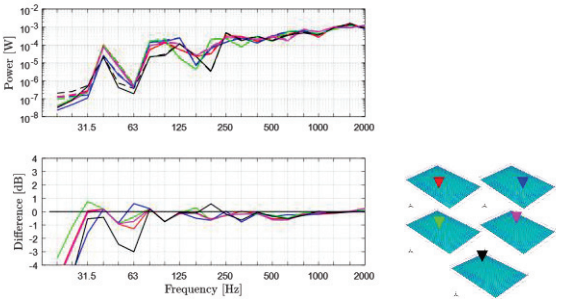

Figure 8: FEM FFFF: direct injected power – solid lines, reception plate power – dashed lines (upper graph), direct injected power minus reception plate power (lower graph).

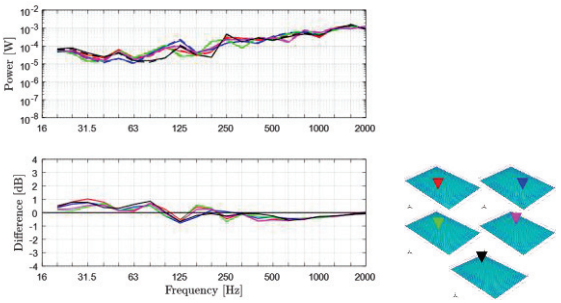

Figure 9: FEM Sylomer: direct injected power – solid lines, reception plate power – dashed lines (upper graph), direct injected power minus reception plate power (lower graph).

Sampling strategy for reception plate approach

Although the viscoelastic material provides some restraint at the plate boundaries, the vibration levels near corners still tend to be large compared to the central zone of the plate. Although it is quick with FEM to sample the velocity in a regular grid over the entire plate surface, it is less convenient with laboratory measurements. Therefore, a sampling strategy is required to account for the spatial variation in velocity over the surface of the reception plate. For field measurements of sound insulation, similar issues occurred when measuring the sound pressure level in rooms at low-frequencies; the solution adopted was to sample the sound pressure in corners as well as the central zone and combine them with an empirical equation that gave a good estimate of the room average sound pressure level [10]. A similar

approach is considered here by introducing a weighting factor, X, to combine velocity measurements in the corners and the central zone (0.5 m away from the edges) of the plate. This gives a spatial average velocity level using

$$L_v = 10\lg\left[\frac{X\cdot 10^{L_{\text{CentralZone}}/10} + 10^{L_{\text{Corner}}/10}}{X+1}\right] \quad (4)$$

The proposal for X is indicated in Figure 10. The importance of the corner is clear from $X = 1$ at frequencies up to 40 Hz. At 50 Hz $X = 2$ and then increases by 3 per doubling of frequency band to account for corners. Using this weighting shows good agreement (± 3 dB) between the direct injected power and reception plate power for all five different excitation positions (see Figure 11).

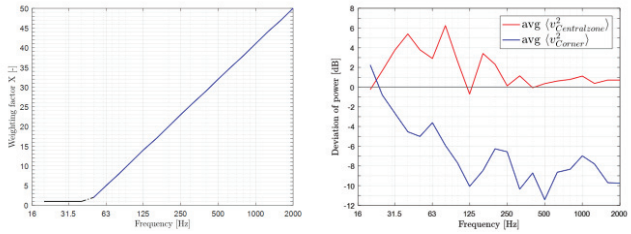

Figure 10: (Left) Weighting factor X for the reception plate power. (Right) Direct injected power minus reception plate power for central zone and corner positions.

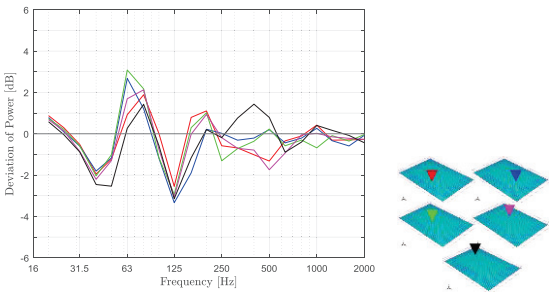

Figure 11: Direct injected power minus reception plate power when using weighting factor X for the reception plate power.

Conclusions

This paper concerns the development of two FEM models of a reception plate (1) an idealised reception plate with free boundary conditions and (2) a realistic reception plate incorporating the viscoelastic material around the boundaries.

The idealised reception plate model shows good agreement in terms of eigenfrequencies and mode shapes at and above 100 Hz whereas the realistic model shows close agreement at all frequencies up to 250 Hz.

The validated FEM model for the realistic reception plate was used to compare the direct injected power and the reception plate power. This showed close agreement (± 1 dB) when the spatial-average velocity was calculated using all elements over the surface of the plate. The model was then used to assess a potential sampling strategy from which the spatial-average velocity could be determined in experimental work where time constraints mean that it is not always possible to samples at all positions in a regular grid over the plate surface. An empirical weighting was used to define a sampling strategy based on measuring at plate corners and the central zone of the plate.

The next stage of the research is to estimate structure-borne sound power from the validated FEM model when compared with measurements on the laboratory heavyweight reception plate. In addition, the effect of commonly found multi-contact and framed sources will be investigated using FEM.

Literature

[1] C. Hopkins, M. Robinson. Using transient and steady-state SEA to assess potential errors in the measurement of structure-borne sound power input from machinery on coupled reception plates, Applied Acoustics 2014, 79, 35-41.

[2] C. Hopkins, M. Robinson. On the evaluation of decay curves to determine structural reverberation times for building elements, Acta Acustica united with Acustica 2013, 99(2), 226-244.

[3] M. M. Späh, B. M. Gibbs. Reception plate method for characterisation of structure-borne sound sources in buildings: Assumptions and application, Applied Acoustics 2009, 70, 361-368.

[4] EN 15657-1: Acoustic properties of building elements and of building – Laboratory measurement of airborne and structure-borne sound from building equipment – Part 1: Simplified cases where the equipment mobilities are much higher than the receiver mobilities, taking whirlpool baths as an example, October 2009.

[5] EN 12354-5: Building acoustics – Estimation of acoustic performance of building from the performance of elements – Part 5: Sound levels due to the service equipment, October 2009.

[6] R. J. M. Craik. The measurement of the material properties of building structures, Applied Acoustics 1982, 15:275-282.

[7] C. Hopkins. Sound insulation, Butterworth-Heinemann 2007, ISBN 978-0-7506-6526-1.

[8] EN 29052-1: Acoustics – Methods for the determination of dynamic stiffness – Part 1: Materials used under floating floors in dwellings, August 1992.

[9] S. Reinhold, C. Hopkins, B. Zeitler. Finite element simulation of a laboratory reception plate for structure-borne sound power measurements, INTER-NOISE 2016, 3734-3742, Hamburg.

[10] C. Hopkins and P. Turner. Field measurement of airborne sound insulation between rooms with non-diffuse sound fields at low frequencies. Applied Acoustics 2005, 66, 1339-1382.